Post-print of: Mielewczyk-Gryń A., Wachowski S., Strychalska-Nowak J., Zagórski K., Klimczuk T., Navrotsky A., Gazda M.: Heat capacities and thermodynamic properties of antimony substituted lanthanum orthoniobates. CERAMICS INTERNATIONAL. Vol. 42, iss. 6 (2016), p. 7054-7059. DOI: 10.1016/j.ceramint.2016.01.093

Heat capacities and thermodynamic properties of antimony substituted lanthanum orthoniobates

Aleksandra Mielewczyk-Gryn[a] Sebastian Wachowski[a], Judyta Strychalska[a], Krzysztof Zagórski[a], Tomasz Klimczuk[a], Alexandra Navrotsky[b], Maria Gazda[a]

[a]Faculty of Applied Physics and Mathematics, Gdansk University of Technology, Narutowicza 11/12, 80-233 Gdansk, Poland
[b]Peter A. Rock Thermochemistry Laboratory and NEAT ORU, University of California Davis, Davis, CA 95616, USA

Abstract

The results of heat capacity measurements for the lanthanum orthoniobate substituted with 10, 20 and 30 mol% of antimony ($LaNb_{0.9}Sb_{0.1}O_4$, $LaNb_{0.8}Sb_{0.2}O_4$ and $LaNb_{0.7}Sb_{0.3}O_4$) are presented and discussed. Temperature dependence of low temperature heat capacity was analyzed within the Debye and Einstein models. The Debye temperature decreased, whereas the Einstein temperature increased with antimony content. The decrease of the Debye temperature with increasing antimony content was correlated with decreasing scheelite–fergusonite transition temperature. The increase of the Einstein temperature of $LaSb_xNb_{1-x}O_4$ with increasing antimony content may indicate increasing frequency of optical vibrations of $Nb(Sb)–O_4^{-2}$ polyhedra relative to La^{3+} cations. Using the heat capacity data, standard entropies of the phases were calculated and combined with previously measured enthalpies of formation to obtain Gibbs energies of formation. Standard thermodynamic properties were tabulated.

Keywords: Lanthanum orthoniobate; Heat capacity; Debye temperature; Entropy; Gibbs energy

1. Introduction

Understanding the thermodynamic properties of ceramic materials operating in a wide temperature range is crucial in terms of applications and from the geochemical point of view. In this work we focus on lanthanum orthoniobates, that is, on compounds based on $LaNbO_4$ stoichiometry. Properties of these materials may be modified by different substitutions. For example, temperature of the structural phase transition from the monoclinic to the tetragonal phase depends on the type and amount of substituting atoms. The phase transition temperature of stoichiometric $LaNbO_4$ is about 770 K [1] but it may be either decreased or increased if Nb is partially substituted by other elements. For instance, substituting niobium by an element with higher ionic radius, such as Ta, leads to increase of the phase transition temperature [2,3]. However, particularly interesting is the possibility of decreasing the transition temperature below room temperature which may be achieved through substitution with antimony or vanadium [4–8]. In our previous work we analyzed the influence of antimony substitution on the spontaneous strain and Landau order parameter [7]. It was shown that the introduction of antimony atoms into the niobium sublattice does not change the nature of the phase transition which is second order. Further investigation by high temperature oxide melt solution calorimetry has allowed us to analyze the energetic stability of materials containing different concentrations of substituent. The investigation showed that the enthalpy of structural phase transition for these compounds is relatively low [7]. In the present work, heat capacity measurements at 2–870 K for lanthanum orthoniobate substituted by 10, 20 and 30 mol% of antimony are presented and discussed. Standard entropies and Gibbs energies of formation are calculated.

http://dx.doi.org/10.1016/j.ceramint.2016.01.093

2. Experimental methods

The $LaNbO_4$, $LaNb_{0.9}Sb_{0.1}O_4$, $LaNb_{0.8}Sb_{0.2}O_4$ and $LaNb_{0.7}Sb_{0.3}O_4$ samples were synthesized as described elsewhere [4]. The sintered samples were crushed into powder and analyzed by powder X-ray diffraction using a Phillips X'Pert Pro MPD diffractometer with Cu K_α radiation. Single phase pulverized samples were then analyzed in order to determine their high temperature heat capacity. Heat capacity at high temperature (350–870 K) was measured by a Setaram LabSY-Sevo system. Measurements were undertaken in Pt crucibles; the system was calibrated by Al_2O_3 prior measurements and purged by argon during measurements. Heat capacity measurements (thermal relaxation technique) in the temperature range $2 < T < 300$ K were carried out using a Quantum Design Physical Property Measurement System (PPMS). The accuracy of C_p measurements was established to be approximately 3% and 0.5% at high (LabSYSEvo) and low (PPMS system) temperatures, respectively. All errors of calculated values were calculated by error propagation.

3. Results and discussion

The low and high temperature heat capacities are depicted in Fig. 1. All heat capacity vs. temperature curves are similar. Below 300 K (Fig. 1a) heat capacity monotonically increases with temperature, whereas in the high temperature range it first slowly increases and above 550 K it may decrease slightly (Fig. 1b). An average value of C_p between 400 K and 900 K is close to the Dulong and Petit $3nR$ value, where R is the gas constant and n is the number of atoms in the formula unit, namely six for $LaNb_{1-x}Sb_xO_4$. A possible small decrease of heat capacity above 550 K may be caused by a loss of gases ($< 5\%$ total weight loss) from the material, and is not considered significant within the error of DSC measurements. Indeed water and carbon dioxide desorption from $La_{0.98}Mg_{0.02}NbO_4$ in argon atmosphere was observed at 633, 733 and 948 K [9]. Sarin et al. also observed a weak decrease of C_p in high temperatures in rare earth orthoniobates [10].

In order to study the influence of the antimony substitution on heat capacity of $LaNb_{1-x}Sb_xO_4$ the temperature dependence of heat capacity in the low temperature range was analyzed. In general, heat capacity includes contributions from electronic, harmonic, dilatational and anharmonic terms. In the present analysis corrections for dilatation and anharmonicity were not included. Low temperature heat capacity temperature dependence was analyzed in two steps. First, the data below approximately 8 K were fitted with Eq. (1)

$$C_p = \gamma T + \beta T^3 \tag{1}$$

where the first and the second terms correspond to the electronic and phonon contributions to the specific heat, respectively. The value of β parameter of the phonon term, described by Eq. (2), allows determining the Debye temperature (θ_D).

$$\beta = \frac{12\pi^4}{5\theta_D^3} nR, \quad n = 6 \tag{2}$$

The second step of the data analysis was performed in the temperature range 2–300 K. In this case the contribution of optical phonons should be also taken into account, so that, the phonon heat capacity was treated as the sum of Debye and Einstein terms. The following formula was used:

$$C_p = \gamma T + kC_{Debye} + (1-k)C_{Einstein} \tag{3}$$

where k is the weight of the Debye term. Debye and Einstein heat capacities are described by Eqs. (4) and (5).

$$C_{Debye} = 9nR\left(\frac{T}{\theta_D}\right)^3 \int_0^{x_D} \frac{x^4 e^x}{(e^x-1)^2} dx \tag{4}$$

$$C_{Einstein} = 3nR\left(\frac{\theta_E}{T}\right)^2 e^{\frac{\theta_E}{T}} \left(e^{\frac{\theta_E}{T}} - 1\right)^2 \tag{5}$$

where θ_D and θ_E are the Debye and Einstein temperatures, respectively, n is the number of atoms in the formula unit

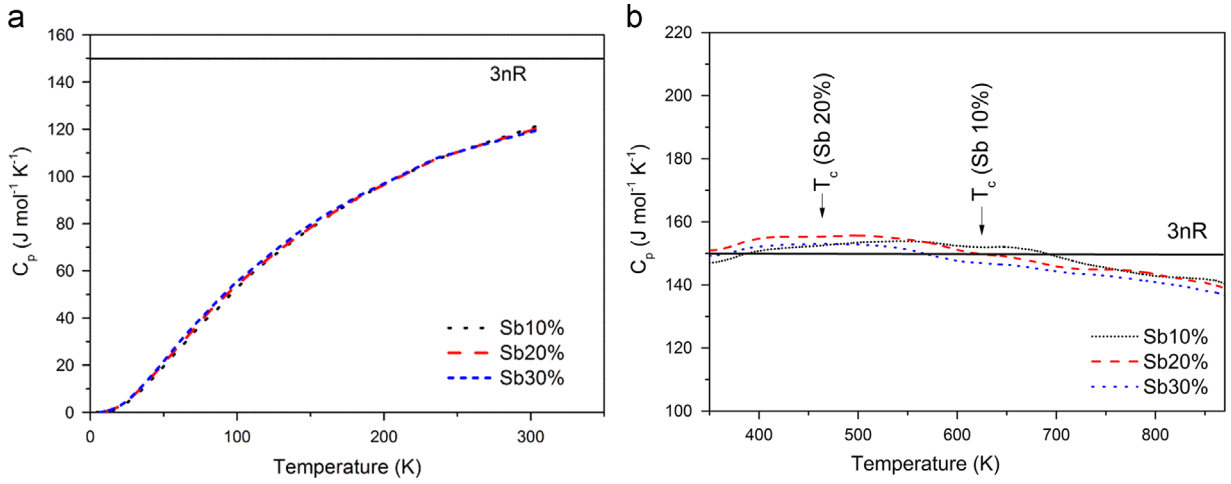

Fig. 1. Temperature dependence of heat capacity of $LaNb_{0.9}Sb_{0.1}O_4$, $LaNb_{0.8}Sb_{0.2}O_4$ and $LaNb_{0.7}Sb_{0.3}O_4$ samples in low (a) and high (b) temperature ranges. T_c (Sb 10%) and T_c (Sb 20%) are temperatures of the scheelite–fergusonite phase transition of $LaNb_{0.9}Sb_{0.1}O_4$, $LaNb_{0.8}Sb_{0.2}O_4$ respectively.

(6) and x_D is θ_D/T. The Debye temperatures and γ parameters determined in the first step of low temperature analysis were used as starting parameters. The three acoustic or optical branches were considered as degenerate.

The fitting of the low temperature heat capacity is shown in Fig. 2, where heat capacity divided by temperature is plotted as a function of T^2. In agreement with relation (1), the plots are linear for temperature below approximately 8 K. The lines intercept the zero point, which means that the γ parameters are small: 0.19 ± 0.10, 0.0 ± 0.1, 0.01 ± 0.04, and 0.36 ± 0.05 mJ mol^{-1} K^{-2} for $LaNbO_4$, $LaNb_{0.9}Sb_{0.1}O_4$, $LaNb_{0.8}Sb_{0.2}O_4$ and $LaNb_{0.7}Sb_{0.3}O_4$, respectively. This confirms that these materials are electronic insulators and the electronic contribution to the heat capacity is negligible. The slopes of the lines as well as the temperature range in which the plots are linear depend on the antimony content. Table 1 summarizes the values of Debye temperature. θ_D decreases with increasing antimony content. The larger atomic mass of antimony than that of niobium could be responsible for this decrease. However, a decrease of Debye temperature has been observed previously by Nevitt and Knapp for vanadium substituted lanthanum orthoniobate [11], despite the lower atomic mass of V than that of Nb, so some other factors may also contribute to the changes with dopant. Low temperature heat capacity is dominated by acoustic phonon modes. Moreover, it has been reported that the scheelite–fergusonite phase transition is associated with acoustic phonon mode softening in the scheelite phase [12]. Raman scattering studies showed that the force constant between the nearest $(Nb,V)O_4$ tetrahedral units softens at T_c as a function of vanadium content [13]. Therefore, as suggested by Nevitt and Knapp, decreasing Debye temperature with increasing vanadium content in $LaNb_{1-x}V_xO_4$ indicates an increase in the low temperature acoustic phonon density of states, which may be associated with a decreasing structural phase transition temperature [6]. In the present study of antimony substituted lanthanum orthoniobate, similar tendencies, namely a decrease of both Debye and transition temperatures with increasing antimony content, are observed. Fig. 3 shows the relation between Debye temperature and the scheelite–fergusonite transition temperatures in both vanadium and antimony substituted lanthanum orthoniobates.

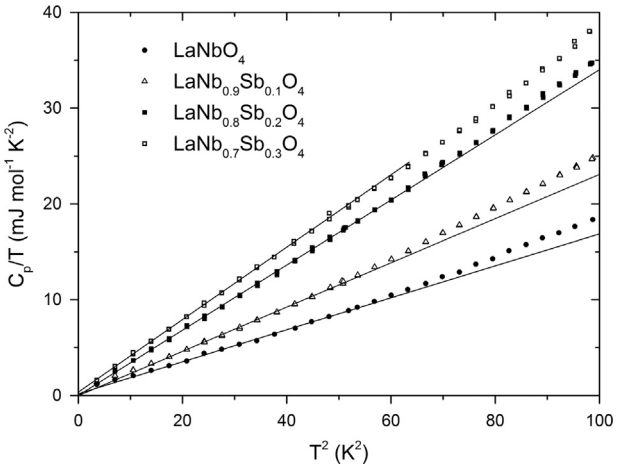

Fig. 2. The heat capacity divided by temperature plotted as a function of T^2. Solid lines correspond to the low temperature fitting by Eq. (1).

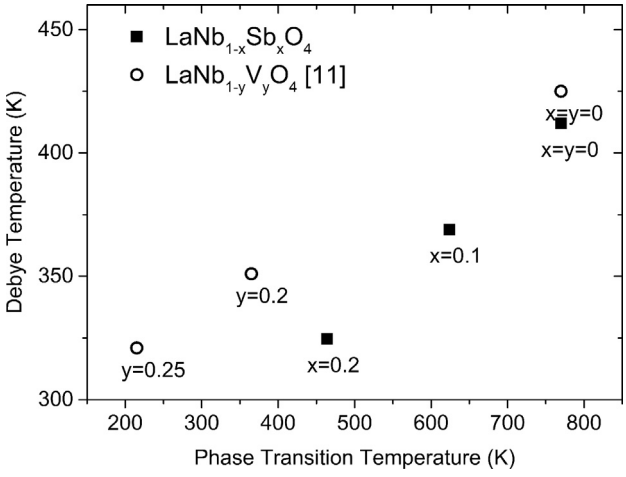

Fig. 3. Debye temperature of $LaNb_{1-x}Sb_xO_4$ ($x=0$, 0.1 and 0.2) and of $LaNb_{1-y}V_yO_4$ ($y=0$, 0.2, and 0.25) [11] plotted versus the scheelite–fergusonite transition temperatures.

Table 1
Debye (determined from fitting the data to Eq. (1) below 10 K) and Einstein (from fitting the data to Eq. (3) below 300 K) temperatures of antimony substituted lanthanum orthoniobates. The k parameter is the weight of the Debye term. For comparison also the Debye temperatures of vanadium substituted materials are given.

Composition	Debye temperature θ_D (K)	Einstein temperature θ_E (K)	k	Reference
$LaNbO_4$	412 ± 2	670 ± 3	0.49 ± 0.01	This work
$LaNbO_4$	425 ± 2	–		[11]
$LaNb_{0.9}Sb_{0.1}O_4$	369 ± 1	672 ± 4	0.48 ± 0.02	This work
$LaNb_{0.8}Sb_{0.2}O_4$	325 ± 2	685 ± 5	0.48 ± 0.01	This work
$LaNb_{0.7}Sb_{0.3}O_4$	313 ± 1	700 ± 6	0.50 ± 0.01	This work
$LaNb_{0.8}V_{0.2}O_4$	351 ± 2	–		[11]
$LaNb_{0.75}V_{0.25}O_4$	321 ± 1	–		[11]

Although the data points for antimony substituted lanthanum orthoniobate fall slightly below those of vanadium substituted compounds, the relations between θ_D and transition temperature are qualitatively similar. This similarity between $LaNb_{1-x}V_xO_4$ and $LaNb_{1-x}Sb_xO_4$ supports the interpretation given by Nevitt and Knapp. The lower values of θ_D of antimony substituted lanthanum orthoniobate in comparison with vanadium substituted compounds are most probably caused by the lower atomic mass of vanadium than of antimony.

An example of the fitting of the high temperature heat capacity, performed with the use of Eq. (3), is depicted in Fig. 4. The Debye contribution calculated from Eq. (4) using the Debye temperature determined on the basis of low temperature data does not describe the total heat capacity above approximately 70 K. The presence of higher energy optical modes is then represented by the Einstein term. The Einstein temperatures determined on the basis of the fitting are collected in Table 1.

In contrast to the Debye temperature, the Einstein temperature of $LaNb_{1-x}Sb_xO_4$ increases with increasing antimony content. The optical phonon modes which are responsible for the Einstein temperature are probably not relevant for the structural transformation of lanthanum orthoniobate [11].

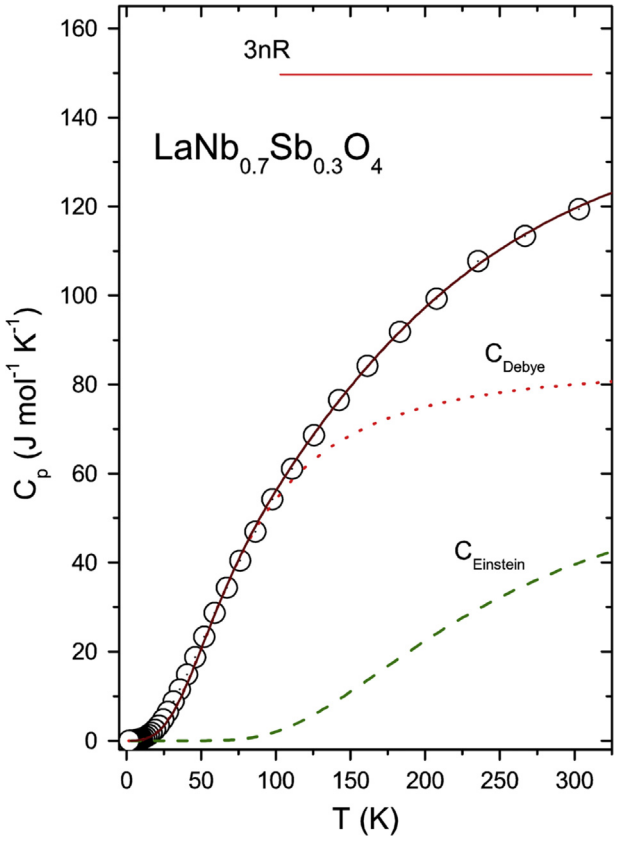

Fig. 4. The heat capacity vs. temperature for $LaNb_{0.7}Sb_{0.3}O_4$. Points represent measured heat capacity whereas the solid black curve is the fit to the measured data (Eq. (3)). Dashed and dotted lines correspond to the Debye and Einstein parts of the total heat capacity, respectively.

Direct information concerning optical phonon characteristics of lanthanum orthoniobate is scarce; however, similar compounds, i.e. $SrWO_4$, $CaWO_4$, $SrMoO_4$ and $CaMoO_4$, have been studied [14,15]. Senyshyn et al. analyzed contributions of particular atoms to the $CaMoO_4$ phonon density of states and showed that molybdenum and oxygen atoms dominate both the low-frequency lattice modes and the internal modes of MoO_4^{-2} polyhedra, whereas calcium dominates the intermediate frequency region of the phonon spectrum [14]. Porto et al. showed that the wave numbers of optical phonon modes related to the low-frequency external vibrations in which the W(Mo)–O_4^{-2}ox ions move as rigid units are between 75 and 219 cm^{-1}, whereas those of internal W(Mo)–O_4^{-2} unit vibrations are between 202 and 925 cm^{-1} [15]. Assuming that lanthanum orthoniobate has similar vibrational properties as these ABO_4 compounds described above, at temperature below 300 K external vibrations should make the major contribution to the heat capacity, but also a contribution of internal modes may be expected. In the studied niobates the external and internal vibrations are those of the Nb(Sb)–O_4^{-2} polyhedra relative to La^{+3} cations and the internal vibrations of the Nb(Sb)–O_4^{-2} polyhedra, respectively. This means that in both cases a decrease of frequency related to the increasing mass of the vibrating entities could be expected. The observed opposite tendency may indicate that hardening of the force constant between Nb(Sb)–O_4^{-2} anion and La^{+3} cation occurs as a result of increasing antimony content.

In the high temperature range, heat capacity of antimony substituted lanthanum orthoniobates depends weakly on temperature. As seen in Fig. 1b, no change of heat capacity at temperature of the phase transition can be observed. This indicates that the enthalpy and any change in heat capacity associated with the scheelite–fergusonite transition is very low. Nevitt and Knapp found no measurable change in heat capacity at the transition temperature of either pure $LaNbO_4$ or vanadium substituted lanthanum orthoniobate [11]. On the other hand, Sarin et al. reported a 4% step in C_p around the transition temperature of $LaNbO_4$, $YNbO_4$ and $DyNbO_4$ [10]. The low value of heat capacity change or phase transition enthalpy in the scheelite–fergusonite transition is consistent with our previous results on lanthanum orthoniobate where the difference between the enthalpies of formation of the monoclinic and tetragonal orthoniobates has been found to be very low [7]. Similar to high temperature measurements, C_p in the low temperature region shows no detectable transition for the sample with 30 mol% doping, which presumably undergoes such a transition below room temperature.

Once fits to heat capacities were determined, smoothed heat capacities and thermodynamic data were generated for the range of temperature of 2–300 K and are presented in Table 2. Using values of enthalpies of formation from our previous work [7], standard molar entropies, enthalpies and Gibbs energies of formation from oxides and elements are given in Table 3. The thermodynamic parameters for all three compositions are similar with a slight rise of standard entropy with increasing antimony content.

Table 2
Standard thermodynamic functions, heat capacity, heat content and standard entropy at given temperature, for antimony doped lanthanum orthoniobates from 2 to 300 K.

	$LaNb_{0.9}Sb_{0.1}O_4$			$LaNb_{0.8}Sb_{0.2}O_4$			$LaNb_{0.7}Sb_{0.3}O_4$		
T K	$C_{p,m}^{\circ}$ J/mol K	$\Delta_0^T H_m^{\circ}$ kJ/mol	$\Delta_0^T S_m^{\circ}$ J/mol K	$C_{p,m}^{\circ}$ J/mol K	$\Delta_0^T H_m^{\circ}$ kJ/mol	$\Delta_0^T S_m^{\circ}$ J/mol K	$C_{p,m}^{\circ}$ J/mol K	$\Delta_0^T H_m^{\circ}$ kJ/mol	$\Delta_0^T S_m^{\circ}$ J/mol K
2	0.0030	$3x10^{-6}$	0.0021	0.0032	$3x10^{-6}$	0.0023	0.0038	$3x10^{-6}$	0.0025
3	0.0074	$8\ x10^{-6}$	0.0041	0.0098	$9.6x10^{-5}$	0.0047	0.0116	$1.1x10^{-5}$	0.0054
4	0.0152	$2x10^{-6}$	0.0072	0.0215	$2.5x10^{-5}$	0.0090	0.0258	$3.0x10^{-5}$	0.0106
5	0.0286	$4x10^{-6}$	0.0120	0.0426	$5.7x10^{-5}$	0.0157	0.0487	$6.7x10^{-5}$	0.0187
6	0.0494	$8.0x10^{-5}$	0.0190	0.0728	$1x10^{-4}$	0.0263	0.0839	$1x10^{-4}$	0.0305
7	0.0805	$1.4x10^{-4}$	0.0288	0.1157	$1x10^{-4}$	0.0406	0.1313	$1x10^{-4}$	0.04688
8	0.1220	$2.4x10^{-4}$	0.0422	0.1748	$4x10^{-4}$	0.0598	0.1935	$4x10^{-4}$	0.0683
9	0.1793	$4.0x10^{-4}$	0.0598	0.2544	$6x10^{-4}$	0.0848	0.2779	$6.4x10^{-4}$	0.0959
10	0.2517	$6.1x10^{-4}$	0.0823	0.3522	$9x10^{-4}$	0.1166	0.3870	$9.7x10^{-4}$	0.1307
15	0.8954	0.0033	0.2898	1.1699	0.0044	0.3943	1.2413	0.0048	0.4285
20	2.1747	0.0107	0.7074	2.6196	0.0137	0.9145	2.7685	0.0146	0.9808
25	4.0894	0.0261	1.3871	4.7609	0.0318	1.7135	4.9666	0.0336	1.8217
30	6.6280	0.0527	2.3492	7.4732	0.0623	2.8171	7.7708	0.0653	2.9667
35	9.5462	0.0930	3.5856	10.4902	0.1070	4.1905	10.9132	0.1119	4.3972
40	12.7459	0.1486	5.0667	13.8421	0.1677	5.8073	14.3576	0.1750	6.0763
45	16.1262	0.2207	6.7619	17.3000	0.2456	7.6367	17.9497	0.2557	7.9739
50	19.6018	0.3101	8.6399	20.8051	0.3408	9.6403	21.6258	0.3546	10.0544
55	23.0589	0.4168	10.6710	24.3589	0.4537	11.7891	25.4133	0.4721	12.2912
60	26.4649	0.5406	12.8240	27.9156	0.5844	14.0620	29.2297	0.6088	14.6677
65	29.7695	0.6812	15.0727	31.3090	0.7325	16.4304	32.7893	0.7638	17.1478
70	33.2960	0.8386	17.4043	34.8551	0.8977	18.8779	36.2586	0.9366	19.7061
75	37.0006	1.0144	19.8278	38.5210	1.0812	21.4077	39.6593	1.1263	22.3236
80	39.9954	1.2073	22.3165	41.9376	1.2825	24.0045	42.9219	1.3329	24.9883
85	42.7770	1.4142	24.8247	45.2849	1.5005	26.6474	46.1447	1.5555	27.6871
90	46.0585	1.6360	27.3589	48.2566	1.7346	29.3225	49.3134	1.7942	30.4147
95	49.5255	1.8749	29.9420	51.1075	1.9830	32.0079	52.4636	2.0487	33.1654
100	52.7955	2.1310	32.5684	53.9130	2.2456	34.7013	55.3835	2.3186	35.9338
110	58.7978	2.6889	37.8818	59.4165	2.8123	40.0979	60.6488	2.8988	41.4594
120	63.9130	3.3029	43.2205	64.5396	3.4322	45.4887	65.7396	3.5308	46.9554
130	68.7875	3.9668	48.5322	69.4004	4.1025	50.8517	70.6504	4.2132	52.4149
140	73.4610	4.6781	53.8010	73.9693	4.8194	56.1620	75.3511	4.9432	57.8227
150	77.8624	5.4350	59.0216	78.2970	5.5810	61.4149	79.5519	5.7183	63.1687
160	82.1782	6.2352	64.1845	82.5473	6.3852	66.6038	83.5961	6.5340	68.4320
170	86.0857	7.0768	69.2855	86.3879	7.2302	71.7252	87.2079	7.3884	73.6103
180	89.9231	7.9569	74.3147	90.1583	8.1129	76.7698	90.7455	8.2781	78.6951
190	93.3052	8.8737	79.2710	93.4194	9.0316	81.7360	93.9302	9.2020	83.6897
200	96.4859	9.8227	84.1378	96.4520	9.9809	86.6049	96.9566	10.1565	88.5847
210	99.6220	10.8034	88.9221	99.5040	10.9607	91.3843	99.9870	11.1412	93.3885
220	102.6171	11.8146	93.6256	102.6193	11.9713	96.0852	103.0305	12.1563	98.1101
230	105.6122	12.8557	98.2532	105.7345	13.0130	100.7155	106.0739	13.2018	102.757
240	108.1926	13.9258	102.8073	108.3120	14.0847	105.2761	108.5490	14.2764	107.3304
250	110.2847	15.0182	107.2663	110.2510	15.1775	109.7370	110.3456	15.3709	111.7980
260	112.3768	16.1315	111.6325	112.1900	16.2897	114.0989	112.1422	16.4833	116.1609
270	114.4371	17.2657	115.9127	114.0894	17.4213	118.3691	113.8952	17.6137	120.4266
273	115.0347	17.6099	117.1805	114.6330	17.7644	119.6328	114.3921	17.9561	121.6879
280	116.4289	18.4200	120.1105	115.9015	18.5712	122.5510	115.5517	18.7609	124.5987
290	118.4207	19.5942	124.2309	117.7137	19.7393	126.6498	117.2082	19.9247	128.6824
298	120.0141	20.5480	127.475	119.1634	20.6870	129.8727	118.5334	20.8677	131.8899
300	120.4125	20.7884	128.2791	119.5259	20.9255	130.6710	118.8647	21.1051	132.6839

4. Conclusions

The heat capacity of the lanthanum orthoniobate substituted with 10%, 20% and 30% of antimony was measured in the temperature ranges 2–300 K and 350–870 K. The Debye and Einstein temperatures were determined on the basis of the heat capacity temperature dependence below 300 K. A decrease of the Debye temperature with increasing antimony content was correlated with decreasing scheelite–fergusonite transition temperatures. The observed increase of the Einstein temperature of $LaSb_xNb_{1-x}O_4$ with increasing antimony content may be caused by an increase in the frequency of vibrations in

Table 3
Thermodynamic parameters of formation from oxides (*f,ox*) and elements (*f*) at 298 K for lanthanum orthoniobates.

Sample	$\Delta H_{f,ox}$ (kJ/mol) [7]	$\Delta G^0_{f,ox}$ (kJ/mol)	S^0 (J/molK)	ΔH_f (kJ/mol)	ΔG^0_f (kJ/mol)
$LaNb_{0.9}Sb_{0.1}O_4$	-132.85 ± 1.53	-131.34 ± 2.40	127.47 ± 0.43	-1706.90 ± 2.53	-1553.19 ± 29.58
$LaNb_{0.8}Sb_{0.2}O_4$	-132.01 ± 1.53	-131.20 ± 2.40	129.87 ± 0.44	-1707.75 ± 2.54	-1550.48 ± 29.58
$LaNb_{0.7}Sb_{0.3}O_4$	-126.41 ± 1.54	-126.21 ± 2.40	131.88 ± 0.45	-1713.34 ± 2.54	-1552.40 ± 29.58

which the Nb(Sb)–O_4^{-2} oxyions move as rigid units. There is no observable change in the heat capacity at the scheelite–fergusonite transition, consistent with previously measured heats of formation which suggest a very small enthalpy of transformation.

Acknowledgments

The research performed at Gdansk University of Technology was financially supported by the National Science Center (Poland) Grant no. DEC-2012/07/E/ST3/00584. Sample preparation and other work at UC Davis was supported by the U.S. National Science Foundation (grant EAR 13–21410).

References

[1] W.M. Kriven, P. Sarin, L.F. Siah, Phase transformations in rare earth niobates, solid–solid phase transform, Inorg. Mater. (2005) 1015–1022.
[2] F. Vullum, F. Nitsche, S.M. Selbach, T. Grande, Solid solubility and phase transitions in the system $LaNb_{1-x}Ta_xO_4$, J. Solid State Chem. 181 (2008) 2580–2585, http://dx.doi.org/10.1016/j.jssc.2008.06.032.
[3] A.B. Santibáñez-Mendieta, E. Fabbri, S. Licoccia, E. Traversa, Tailoring phase stability and electrical conductivity of $Sr_{0.02}La_{0.98}Nb_{1-x}Ta_xO_4$ for intermediate temperature fuel cell proton conducting electrolytes, Solid State Ion. 216 (2012) 6–10, http://dx.doi.org/10.1016/j.ssi.2011.09.019.
[4] S. Wachowski, A. Mielewczyk-Gryn, M. Gazda, Effect of isovalent substitution on microstructure and phase transition of $LaNb_{1-x}M_xO_4$ (M=Sb, V or ta; x=0.05 to 0.3), J. Solid State Chem. 219 (2014) 201–209 ⟨http://www.sciencedirect.com/science/article/pii/S0022459614003466⟩.
[5] A. Mielewczyk-Gryn, K. Gdula, T. Lendze, B. Kusz, M. Gazda, Nano- and microcrystals of doped niobates, Cryst. Res. Technol. 45 (2010) 1225–1228, http://dx.doi.org/10.1002/crat.201000378.
[6] A. Mielewczyk-Gryn, K. Gdula-Kasica, B. Kusz, M. Gazda, High temperature monoclinic-to-tetragonal phase transition in magnesium doped lanthanum ortho-niobate, Ceram. Int. 39 (2013) 4239–4244, http://dx.doi.org/10.1016/j.ceramint.2012.09.102.
[7] A. Mielewczyk-Gryn, S. Wachowski, K.I. Lilova, X. Guo, M. Gazda, A. Navrotsky, Influence of antimony substitution on spontaneous strain and thermodynamic stability of lanthanum orthoniobate, Ceram. Int. 41 (2015) 2128–2133, http://dx.doi.org/10.1016/j.ceramint.2014.10.010.
[8] A.D. Brandão, I. Antunes, J.R. Frade, J. Torre, V.V. Kharton, D.P. Fagg, Enhanced Low-temperature proton conduction in $Sr_{0.02}La_{0.98}NbO_{4-\delta}$ by scheelite phase retention, Chem. Mater. 22 (2010) 6673–6683 http://dx.doi.org/10.1021/cm102705e.
[9] A. Mielewczyk-Gryn, S. Wachowski, K. Zagórski, P. Jasiński, M. Gazda, Characterization of magnesium doped lanthanum orthoniobate synthesized by molten salt route, Ceram. Int. 41 (2015) 7847–7852, http://dx.doi.org/10.1016/j.ceramint.2015.02.121.
[10] P. Sarin, R.W. Hughes, D.R. Lowry, Z.D. Apostolov, W.M. Kriven, High-temperature properties and ferroelastic phase transitions in rare-earth niobates ($LnNbO_4$), J. Am. Ceram. Soc. (2014) 3319 http://dx.doi.org/10.1111/jace.13095.
[11] M.V. Nevitt, G.S. Knapp, Phonon properties of vanadium-substituted lanthanum niobate derived from heat-capacity measurements, J. Phys. Chem. Solids. 47 (1986) 501–505, http://dx.doi.org/10.1016/0022-3697(86)90049–1.
[12] K. Parlinski, Y. Hashi, S. Tsunekawa, Y. Kawazoe, Computer simulation of ferroelastic phase transition in $LaNbO_4$, J. Mater. Res. 12 (1997) 2428–2437, http://dx.doi.org/10.1557/JMR.1997.0321.
[13] A.T. Aldred, S.-K. Chan, M.H. Grimsditch, M.V. Nevitt, Displacive phase transformation in vanadium-substituted lanthanum niobate, MRS Proc. 24 (1983).
[14] A. Senyshyn, H. Kraus, V. Mikhailik, L. Vasylechko, M. Knapp, Thermal properties of $CaMoO_4$: lattice dynamics and synchrotron powder diffraction studies, Phys. Rev. B. 73 (2006) 1–9, http://dx.doi.org/10.1103/PhysRevB.73.014104.
[15] S.P.S. Porto, J.F. Scott, Raman spectra of $CaWO_4$, $SrWO_4$, $CaMoO_4$, and $SrMoO_4$, Phys. Rev. 157 (1967) 716–719, http://dx.doi.org/10.1103/PhysRev.157.716.